Proceedings of the 7th International Symposium on Cavitation
CAV2009 – Paper No. 41
August 17-22, 2009, Ann Arbor, Michigan, USA

Cavitation Erosion – A review of physical mechanisms and erosion risk models

Tom J.C. Van Terwisga
MARIN, Delft University of Technology
Wageningen, The Netherlands

Patrick A. Fitzsimmons
Lloyd's Register
London, United Kingdom

Li Ziru
Delft University of Technology
Delft, The Netherlands

Evert Jan Foeth
MARIN
Wageningen, The Netherlands

ABSTRACT

This work aims at a postprocessing procedure for the assessment of the cavitation erosion risk based on multiphase CFD results an on experimental observations. Existing procedures often use available information, such as the rms value of the vapour fraction in a particular area, without thorough justification of this criterion. This paper aims at linking the available information that comes from multiphase RANS or experimental observations with High Speed Video, with the many publications on fundamental mechanisms of cavitation dynamics.

The first objective of this paper is to review physical mechanisms for cavitation erosion loads that have been suggested in the literature. These mechanisms are evaluated with observations that are available from full scale ships where cavitation has lead to erosion damage on the rudder or the propeller.

A second objective is to review risk assessment models that use CFD results or experimental results as input for the prediction of the risk of cavitation erosion.

A detailed phenomenological description of the process leading to cavitation erosion from sheet cavitation and vortex cavitation is hypothesized. The process is based on the conversion of potential energy contained in the cavity and a focusing of this energy in space and in time that is governed by ring vortices or horseshoe vortices in case the ring vortices attach to a surface. It is concluded from experiments by Kawanami etal. [1] that horseshoe vortices tend to concentrate the vorticity toward the material surface. It is hypothesized in this paper that this concentrated vorticity forms a mechanism to break a monolithic cavity up into bubbles due to instabilities caused by the high fluid velocities and to concentrate all microbubbles in space by centrifuging out the heavier liquid particles. The radiated shockwaves caused by the implosion of one microbubble is then hypothesized to be sufficient to initiate a synchronized implosion of the cloud of microbubbles in the immediate vicinity.

A selection of cavitation erosion models available in open literature is reviewed in this paper. It is concluded that the models by Bark et al. [2] and Fortes-Patella et al. [3] appear to offer the best frameworks to be coupled to the mechanisms hypothesized in this paper.

INTRODUCTION

"Rudder cavitation is a long recognized problem in shipping industry. Nevertheless, we are still far away from practical final solutions to improve the situation" (Friesch 2006 [4]). This paper aims to contribute to a solution to the many ship rudder and propeller erosion problems, as they not only increase the maintenance cost but may eventually compromise the safety of the ship. Moreover, design measures to prevent cavitation erosion on propellers are always at the cost of propeller efficiency. It is therefore important to understand the causes of cavitation erosion, and to predict accurately its aggressiveness in terms of erosion risks, or even better, damage rate.

The first objective of this paper is to review physical mechanisms for cavitation erosion loads that have been suggested in the literature. These mechanisms are evaluated with observations on the detailed dynamics of the flow over a cavitating foil, and with observations that are available from ships where cavitation has lead to erosion damage on the rudder or the propeller.

The second objective is to review the risk assessment models that use CFD or experimental results as input for the prediction of the risk of cavitation erosion.

With the advent of multiphase RANS codes for the prediction of the larger scale cavity structures (macro structures, $\mathcal{O}$(0.1 chord length)), the urge for a rational postprocessing for the assessment of the cavitation erosion risk increases. Results from fundamental research on micro scale cavity dynamics (cavity bubble scale, $\mathcal{O}$ (100 – 500 μm) and bubbly cloud cavity dynamics (see e.g. [5]) can now be

linked to the energy cascade associated with the whole process of cavitation erosion.

The relevance of this work is that it proposes a postprocessing procedure for the assessment of the cavitation erosion risk based on multiphase CFD results or on experimental observations. Existing procedures often use available information, such as the RMS value of the vapour fraction in a particular area, without thorough justification of this criterion (see e.g. [6], [7]). This paper aims at linking the available information that comes from multiphase RANS or experimental observations with High Speed Video, with the many publications on fundamental mechanisms of cavitation dynamics. The importance of vortices in this mechanism is explained in this paper.

BASIC PHILOSOPHY

The notion that the aggressiveness of cavitation could be assessed through a consideration of energy conversion was already acknowledged by Hammitt [8]. He postulated that cavitation damage occurred once the potential energy contained in a shed cavity (E_c) exceeded a certain damage threshold E_s . This threshold would essentially be a function of the material properties on which the erosive action takes place, and not of the type of cavitation.

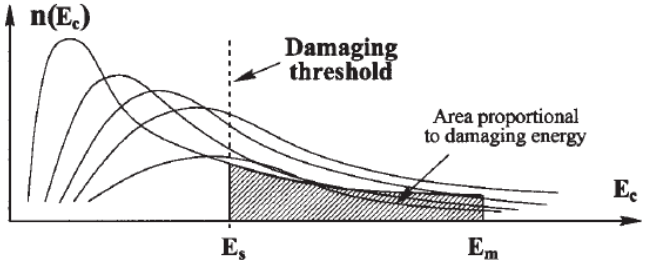

Figure 1: Energy spectra and their relation to cavitation erosion (from [8]).

From energy considerations, one can see that potential energy contained in a macro cavity, is converted into the radiation of acoustic pressure waves, through the conversion of potential into kinetic energy during the collapse phase of the macro scale cavity. This energy cascade was already identified by Fortes-Patella et al. [3].

Energy considerations on the risk of cavitation erosion are also used by Bark et al. [9]: "The concentration or focusing as it is called here, of collapse energy density is most obvious for the spherical collapse with its converging flow. Due to this, the kinetic energy density (the kinetic energy per volume of the liquid) will have a maximum at the cavity interface and this maximum will increase as the collapse proceeds. This is clear already from solution of the Rayleigh-Plesset equation describing this collapse motion. The concept of generalized focusing considers also focusing of energy density for collapses of groups and sequences of cavities." The accumulated kinetic energy is then converted into acoustic energy in the cavity collapse, associated with the shock waves that are radiated by the final collapse.

Franc and Michel [10] estimate the impact pressures and the duration of this impact for four different phenomena associated with different forms of cavity collapse. They distinguish impacts associated with the following phenomena: Micro bubble collapse, an impinging microjet, collective microbubble cloud collapse and impacting cavitating vortices. A review of impact pressures and periods is given inTable 1.

Mechanism	Type of loading	Amplitude [MPa]	Duration [μs]
Micro bubble collapse	pressure wave	100	1
Micro jet (from a 1 mm bubble)	impacting jet	150	0.03
Collective micro bubble collapse	pressure waves	»100	» 1
Cavitating vortices	impacting jet	>100	> 10

Table 1 Review of impact loadings for different cavity phenomena (from Franc and Michel [10])

The pressure amplitude and the duration of the shock wave associated with a single bubble collapse has been measured by Fujikawa et al. [11]. Pressure amplitude and period for a microjet resulting from the collapse of a 1 mm cavity bubble are estimated from pressures found in a water hammer. The duration of the pressure pulse is fixed by the jet diameter d which is of the order of d/2c. For a bubble of 1 mm initial diameter, the jet diameter is about 0.1 mm, which leads to a very small value for the duration of the pressure pulse, i.e. about 0.03 μs. It is thus concluded that the pressure amplitude is of the same order as for an imploding microbubble, but that the duration of the pulse is two orders of magnitude smaller acoustic power release. Implosion of a cloud of microbubbles is typically associated with cascades of implosions. The pressure wave emitted by the collapse and rebound of a particular bubble tends to enhance the collapse velocities of the neighbouring bubbles, thus increasing the amplitude of their respective pressure waves.

"Cavitating vortices appear to be responsible for severe erosion in fluid machinery as described by Oba [12]". Franc and Michel [10] conclude that there are two main features that seem to be at the origin of the potentially highly erosive potential of cavitating vortices. These features are:

- The breaking up of the vortex where the vortex is about to hit the wall, and
- The rather long duration of the impact applied to the wall.

It is concluded from this analysis that the most aggressive acoustic power is emitted from a collective micro bubble collapse, where it will be argued in this paper that cavitating vortices are an effective means to focus the release of acoustic power in space and time, thereby increasing the aggressiveness. It is noted that microbubble cloud collapse and impacting jets are different descriptions for a similar physical phenomenon.

PHYSICAL MECHANISMS LEADING TO CAVITATION EROSION

This section gives a description of the mechanisms that are dominant in converting potential energy as contained in the cavity immediately after it is shed from the sheet, up to the very last stages of the cavity just prior to collapse. An initial distinction will be made between collapse of shed cavities from a sheet and collapse from a cavitating vortex, but it will be argued that the phenomena associated with the final stages before collapse is essentially the same.

SHEET CAVITY COLLAPSE

The following describes the collapse mechanism of a sheet cavity based on a description of flow phenomena as collected from distinct references. Foeth et al [13] have shown that the cloud cavitation that is associated with the break up of sheet cavitation is essentially an organized mixture of cavitating vortices if one has sufficient spatial and temporal resolution when watching this break up process (See Figure 1).

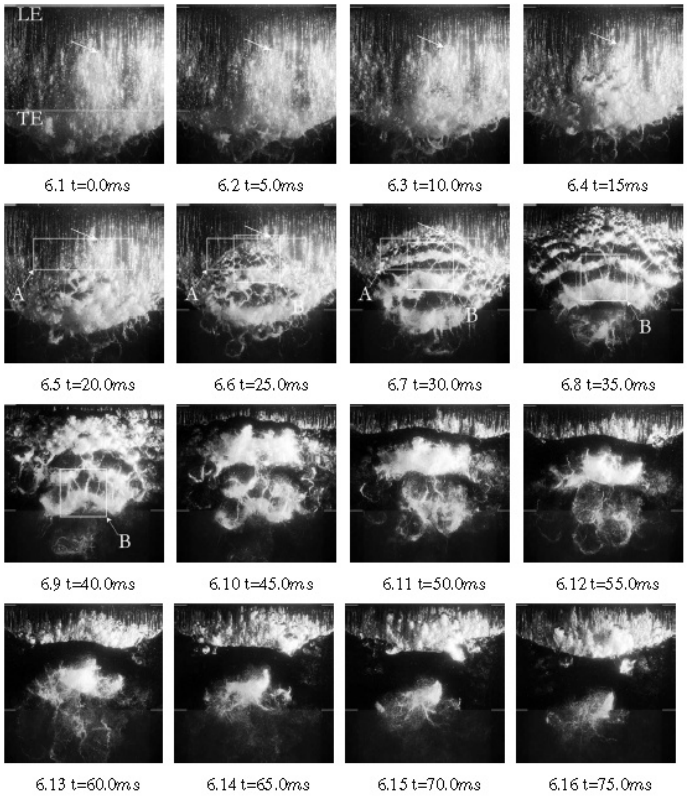

Figure 1: Visualization of a sheet cavity break up into a cloud of cavitating vortices over a twisted foil (from Foeth et al. [13]). The Leading Edge (LE) and trailing edge (TE) are indicated in the first image, mean flow direction is from top to bottom. White outlined area B is enhanced in Figure 2.

A detailed view of the shed "cloud"cavitation is given below, showing the primary spanwise and secondary streamwise cavitating vortices. The streamwise cavitating vortices originate perturbations near the primary spanwise vortices that are stretched around these primary vortices. (from Foeth et al. [13])

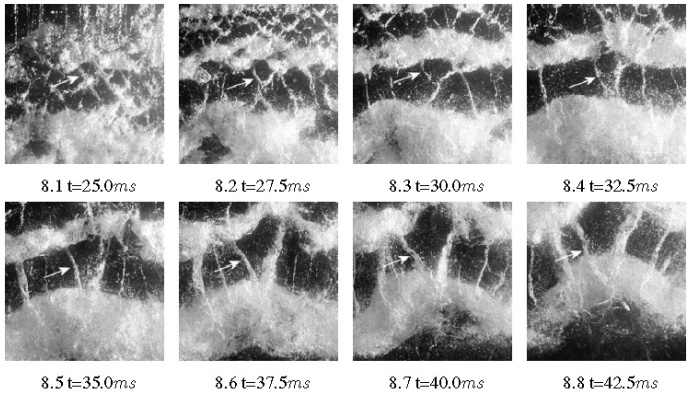

Figure 2 Close up of Figure 1 (detail B) including intermediate images (from Foeth et al. [13]).

The large scale primary spanwise vortices were studied in detail by Pereira et al [14], who observed the development of these vortices with four camera's, observing the shed cavity structures from different viewing angles, thus allowing for a 3D reconstruction of the structures. All cavitating vortices that are produced in the break up region need to be closed vortical structures. These vortices need however not necessarily cavitate over the complete circumference, as the vortex strength may vary. When the vortex loops come close to the material surface, they attach to this surface, the vortices being closed through the boundary layer material. This attachment of the vortex loop to the material surface occurs as a horseshoe vortex, as can clearly be seen from Figure 3.

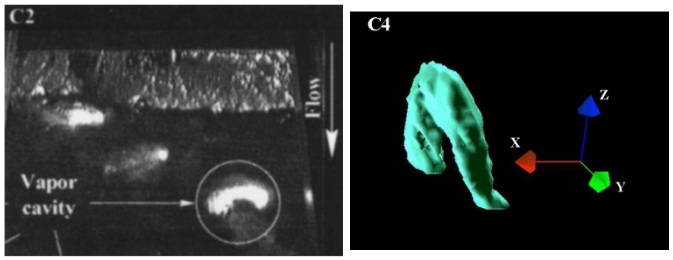

Figure 3 Development of shed cavity structures into a macroscopic body bound cavitating ring vortex (from Pereira etal [14])

Kawanami et al. [1] observed the behavior of shed cavities from a sheet through high speed holography. Their most important result is sketched in Figure 4, where it is shown that the horseshoe vortex occurs as a bubbly cloud. It is furthermore shown that presumably due to self induction, the vorticity is attracted toward the material surface, thereby focusing the bubbly cloud towards the surface. It is consequently the vorticity concentration that focuses the bubble cloud. Although not explained by the authors, the breaking up of the cavitating vortex into bubbles is likely caused by instabilities occurring on the cavity-fluid interface due to the high local fluid velocities.

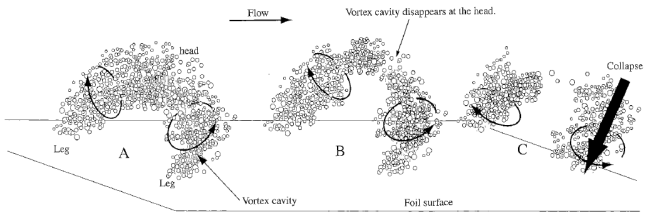

Figure 4 Development of a body attached cavitating ringvortex into a microbubble cloud collapse close to the body. (from Kawanami et al. [1])

The final collapse, possibly followed by one or more rebounds if the energy concentration is sufficiently high, is now triggered by the emission of a shock wave of the first bubble that collapses, thereby synchronizing the collapse of the remaining bubbles.

The mechanism of focussing energy has already been described by Bark et al ([2], [9]). And although the necessary condition of the focussing of the potential energy was clearly described, the focussing mechanism through vortices was not explicitly described. The importance of concentrated vortices on the focussing of energy and ultimately acoustic power release is supported by the results from Schmidt et al. [15], who performed detailed CFD calculations on a twisted hydrofoil. The maximum pressures resulting from one cycle were recorded and are presented for the two alternating shedding cycles found in Figure 5. In both pictures the maximum instantaneous static pressure occurs on the upper surface (suction side) of the hydrofoil, close to the trailing edge. The spanwise position varies from cycle to cycle in an alternating manner. The collapse of the leading edge cavity produces in both cases maximum static pressures of the order of 40 bar (point A). It is seen that the larger shed cavitating vortex (distance between max pressures is highest), also results in the highest pressures (133 bar), which is ascribed here to the larger energy content logically contained in the larger vortex.

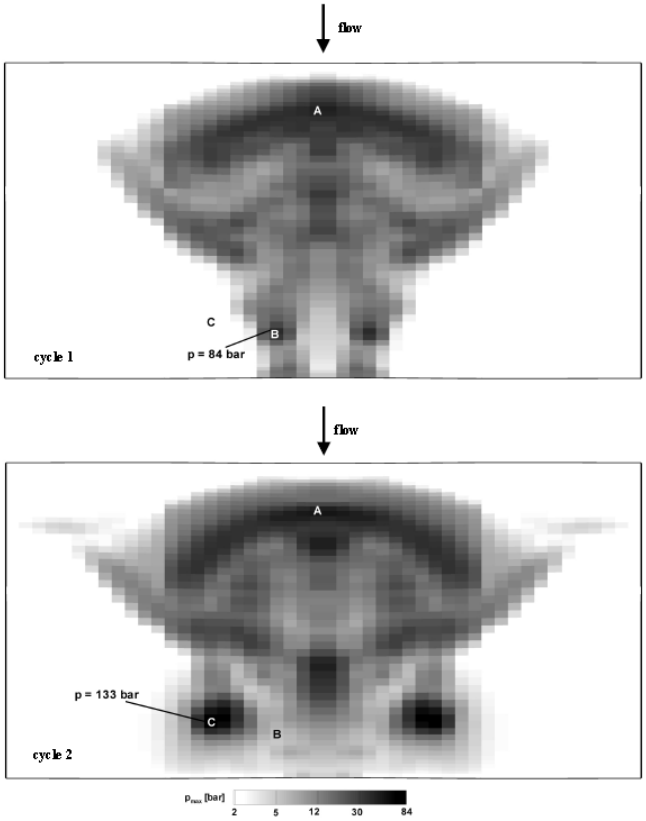

Figure 5 Cell wise recorded maximum static pressure during cycle 1 (top) and during cycle 2 (bottom) caused by sheet cavity shedding over a twisted foil (from Schmidt et al. [15])

VORTEX CAVITY COLLAPSE

A thorough understanding of the erosive action caused by unstable vortex cavitation is hampered by the difficulty of visualizing the hydrodynamics in such a flow and associating this with actual damage on propeller or rudder. As erosive action takes time to become effective, and observations are typically made for limited periods of time, the only way to directly couple flow visualizations with damage areas is through cavitation tunnel experiments using artificial surface treatments which quickly react to erosive action.

The general understanding of erosion by cavitating vortices is that erosive action occurs for cavitating vortices that become unstable and break up. This breaking up of a vortex must necessarily be associated with a redistribution of vorticity, occurring as a branching off in multiple cavitating vortices and/or through the formation of ring vortices around the primary vortex (see Figure 6). It is hypothesized that a stable cavitating vortex aligned along a surface, of e.g. a propeller blade or rudder, is not erosive, because there is no collapse and focusing of cavitation energy. Only if it breaks up in ring vortices that develop into horseshoe vortices once they get attached to the surface, it likely leads to erosion. The aggressiveness being dependent on the potential energy contained in the ring vortex and the effectiveness of focusing of this energy.

Kuiper [16] discusses the difference between vortex bursting and "blowing up" or "breaking up" behavior of a cavitating vortex. The difference between the two mechanisms being that "bursting" is associated with an instability of the vortex core due to e.g. a decrease in axial velocity. It is argued by Kuiper that the break up of a vortex cavity, as for example seen in Figure 6, is caused by the load variation of the blade. The strength of the ring vortices that surround the primary vortex are thus proportional to the blade loading gradient in time $\frac{\partial \Gamma}{\partial t}$, which is entirely governed by the gradient of the axial velocity in the wakefield. Kuiper also states that the breaking up of the cavitating tip vortex does not seem to be a necessary requirement for cavitation erosion on the rudder to occur. There appear to be cases where erosion on the rudder occurred without the tip vortex breaking up. This is however contradictory with the hypothesis that the cavitating vortex should be broken up in order to lead to cavitation erosion.

It is hypothesized here that focusing is a strong function of the vortex strength of this ring vortex. The focusing process being equal to the same process of cavitating vortices produced by shed cavities from sheets, as discussed above.

Figure 6 Breaking up tip vortex cavitation (Friesch [4])

Although the photographs in Figure 7 have little resolution, it appears that the cavitating vortex near the Trailing Edge shows instable behaviour, as can be observed at the letters D and E. If these structures occur close to the blade surface, there is a great risk of cavitation erosion.

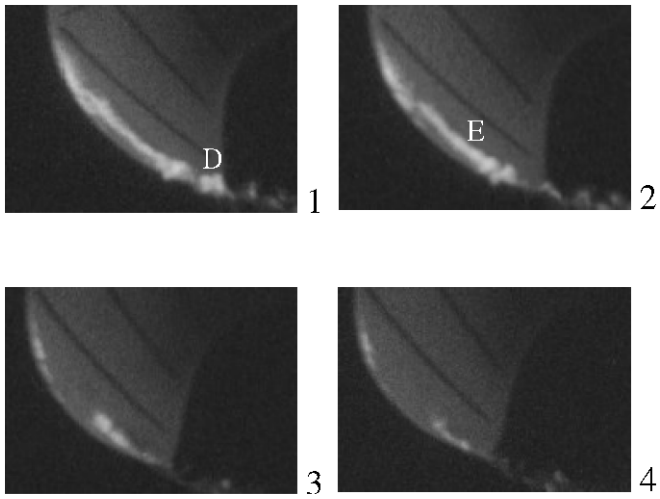

Figure 7 Unstable cavitating Leading Edge vortex leading to cavitation erosion in TE region of tip (Bark et al. [9], EROCAV ship no. 2).

An interesting experimental study of erosion by a cavitating vortex is presented by Moeny et al. [17]. In this study, the erosive behavior of a cavitating vortex along a lifting body is studied. The experimental set-up is shown in Figure 8.

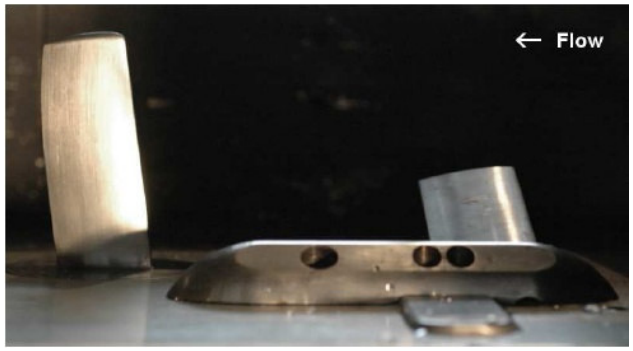

Figure 8 Side view of experimental setup. The test fin is on the left, the vortex generation fin is on the right. Flow is right to left (Moeny et al. [17]).

Figure 9 gives an overview of the cavity events observed and the coating damage that occurred through the erosive action of the shed cavitation. It is interesting to note that there is apparently little or no damage caused by the primary cavitating vortex along the test fin, but that the focus of the erosion damage is in the wake of the induced secondary cavity at the Leading Edge of the foil. Figure 10 shows the cavitating structures for a short exposure time of 1 msec. It can be seen the the primary cavitating vortex shows little tendency to break up, but that small and bright cavitating structures (presumably cavitating vortices) are shed from the secondary cavity at the Leading Edge, which are held responsible for the scattered damage in the wake of this secondary cavity. The scattered character of the shed cavities becomes apparent in Figure 11, where a long exposure time of 50 sec is composed.

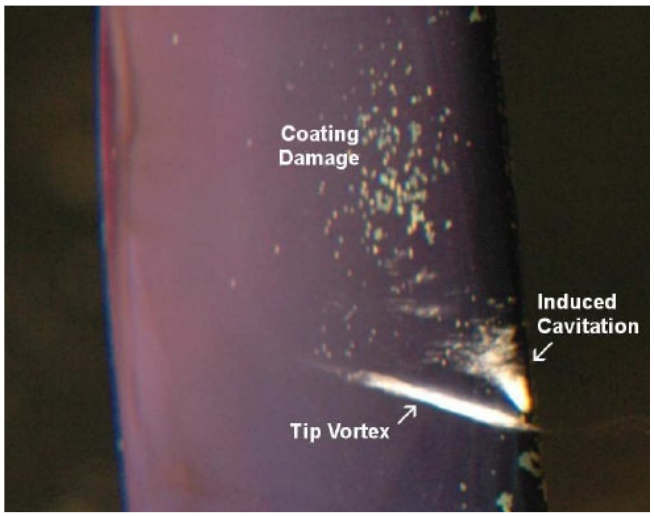

Figure 9 Overview of tip vortex cavity over the test foil with induced cavitation at the leading edge and resulting erosion damage (Moeney et al. [17]).

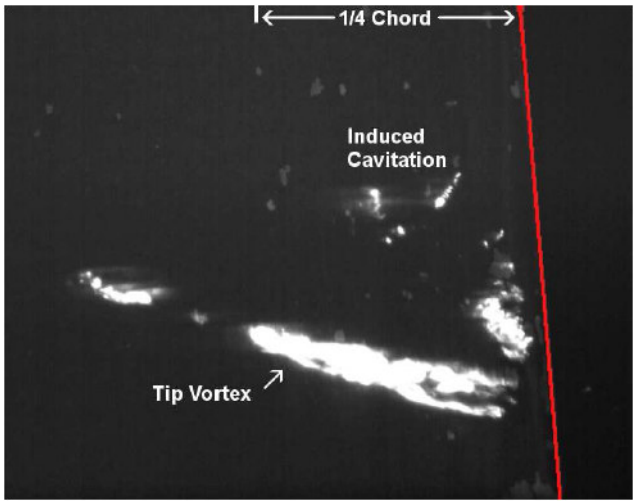

Figure 10 Tip vortex and induced cavitation event with 1.0 msec exposure. The red line indicates the fin leading edge (Moeney et al. [17]).

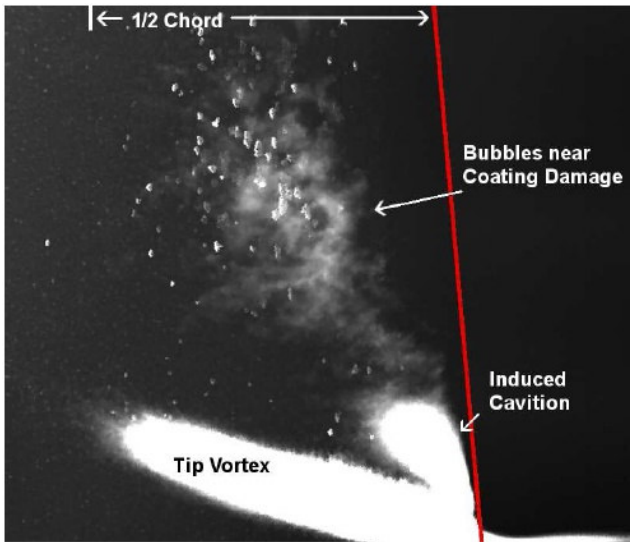

Figure 11 Composite image showing sum of cavitation events over 1000 frames at 20 frames/sec. Leading edge is shown in red (Moeny et al. [17]).

EXAMPLES OF CAVITATION EROSION

As a first test of the usefulness of the sketched mechanism of cavitation erosion in practice, two examples of cavitation erosion on ship rudders and two on ship propellers will be discussed in the following.

Figure 12 shows erosion on a rudder horn operating behind a left-handed CP propeller which was positioned at a minimal distance aft of the propeller plane. In this case, high speed video images from sea trials have clearly identified the cause of the erosion as being the flare-up and collapse of the core of cavitation bubbles within the tip vortex as its free end was dragged across the surface of the horn and through the suction region just behind leading edge on the port side. In this case the vortex had trapped the vapor core, allowing it to react to the ambient flow field created by the swirling slipstream from the propeller. It is conceivable that had the rudder horn been twisted to starboard, the slipstream incident angle would have been reduced and hence the ambient pressure field would have been moderated. This in turn would have moderated the strong adverse influence of the low suction pressure region on the dynamics of the bubbly core of the vortex.

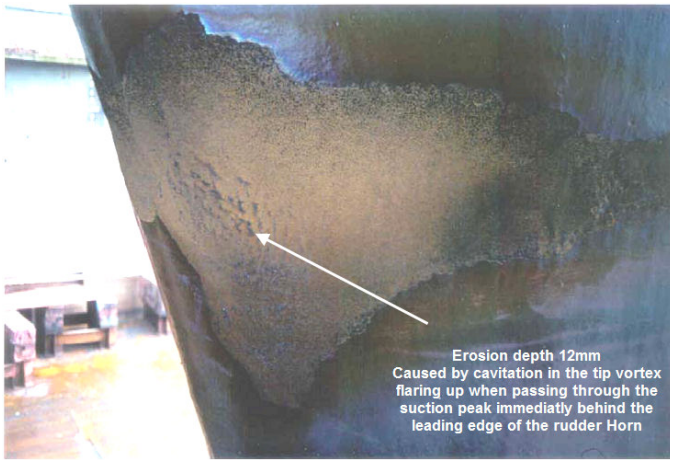

Figure 12 Cavitation erosion damage on a rudder (Courtesy Lloyd's Register)

Figure 13 shows a more conventional rudder horn arrangement for a single screw container ship at its second 5-year dry-docking. Erosion was detected on it and its sister ship at the first 5-year docking and remedial action had to be applied. This consisted of stainless steel plating both covering areas eroded by the propeller tip vortex and also creating "ski-jumps" to deflect cavitation away from the pintle housing.

Figure 13 Cavitation erosion damage on a rudder horn (Courtesy Lloyd's Register)

The tip vortex had eroded some of the welds between the stainless steel plating of both the rudder blade and the rudder horn Cathodic reactions then caused wastage through corrosion and vibration of the plates causing further cracking of plates and welds, leading to a loss of material from the rudder blade. Subsequent sea trials by Lloyd's Register using high speed video cameras, borescopes and acoustic emissions transducers, confirmed that a strong cavitating tip vortex was generating high levels of impulsive cavitation across the damaged region. The moments of impact corresponded with the impingement of that part of the tip vortex that was generated with blade tips in the 12 o'clock position.

Figure 14 shows thick sheet cavitation forming in the root region of a fast patrol craft. This vessel suffered from severe erosion (5mm depth, generated in 30 minutes at sprint speed). The erosion pattern covered the middle 1/3rd of the blade chord just above the root fillet.

Figure 14 Thick sheet cavitation in the root region of a Fast Patrol Craft (Courtesy Lloyd's Register)

The region where the damage was thought to occur (6 o'clock position) could not be viewed, however, the loop and ring vortices shed from the end of the sheet cavity followed the path along which the erosion markings were found. It is conceivable that these well-defined structures carried stable volumes of cavity bubbles downstream into regions of adverse ambient pressure fields where the trapped potential energy could be released onto the blade surface, thus enhancing the erosion effect.

The vessel's problems were only solved when air was injected at several points from under the rope guard, as shown.

The composite image in Figure 15 shows a partly emerged propeller blade with an area of marker paint covering a region of the blade where repairs had been performed. This area had been eroded by tip vortex cavitation streaming aft from one of the pre-swirl vanes shown just ahead of the repaired blade. The insert shows an accurate replica of the eroded area, which included a hole through the blade (see the bulge at the upper right hand end of the moulding.

Figure 15 Composite image of a replica of erosive damage in the Trailing Edge region of the propeller blade, as indicated on the emerged propeller blade with marker paint (Courtesy Lloyd's Register)

The interesting features of this case are

- The cavitating tip vortex from the fin did not erode the blade at any point ahead of the painted area, even although all parts of the blade on radius at which the blade cut through the vortex were in contact with this vortex.
- Consequently the possible growth of cavitation bubbles within the free end of the vortex and the ambient pressure field near the trailing edge of the blade created conditions for the enhanced collapse of the bubble system and erosion of the blade surface.
- Within the replica one can see, from left to right, defined striations, at a near constant pitch, indicating deep and shallow (spanwise) grooves in the blade, culminating in a groove deep enough to cut through the thickness of the blade.
- This last observation suggests that there is a pulsating character to the ambient pressure field such that enhanced collapse occurs only in this region, close to the trailing edge, where one might expect vortex shedding to influence the up-stream ambient pressure field.

The latter case indicates an increase in the aggressiveness of cavitation from a dynamic external pressure field. It is believed that the mechanism for this cyclic external pressure field is an enhancement of the synchronization of cavity collapse.

RISK ASSESSMENT MODELS

A brief review is given in the following on cavitation erosion models that in some way model the characteristic phases in the physical process from cavity macro structure to microbubble cloud collapse. These cavitation models are evaluated on their suitability to fill the gap between CFD results and the risk assessment for erosion by cavitation. Four cavitation erosion models are discussed in the following, the models being found in the following references:

- Kato et al. [18]
- Bark et al. [2]
- Fortes Patella et al. [3]
- Dular et al. [6]

MODEL BY KATO ET AL. (1996)

A scenario for quantitative prediction of the impact force distribution on the solid surface caused by cavitation was proposed by Kato et al. [18]. The prediction follows six phases of cavity development, where it is assumed that the shock wave caused by the collapse of bubbles separated from the sheet cavity is the primary mechanism for erosion. The following characteristic parameters in the process are assessed:

Stage 1: Cavity type and extent
Stage 2: Cavity generation rate
Stage 3: Number and size distribution of cavity bubbles
Stage 4: Characteristics of collapsing bubbles
Stage 5: Impact force/pressure distribution on solid wall due to cavity bubble collapse
Stage 6: Amount of erosion caused by successive impact forces

The first stage, the estimation of cavity type and extent, has been studied extensively. The last stage, solid surface deformation and removal, was studied from a metallurgical viewpoint. It is pointed out that the estimation of impact force distribution or pressure spectrum is key to the prediction of cavitation erosion. These quantities can be measured and correlated directly with the pit distribution. The cavity generation rate was derived from measurement of the air flow rate into a ventilated cavity, with the assumption that the flow rate necessary to maintain a certain length of the cavity should be same as for a vapor cavity (Brennen, 1969; Billet and Weir, 1975). It is discussed in the paper that the behavior of ventilated cavitation is surprisingly similar to that of natural cavitation including the shedding of cloud cavitation.

It is difficult to measure the number and size distribution of cavity bubbles, as their size changes rapidly. However, the number and size distributions of cavity bubbles can be estimated from a measurement of the air bubble distribution downstream of the cavity collapse region, because the air bubbles downstream are "remains" of the cavity bubbles and their distribution should thus be similar (see Figure 16). Diffusion of the gas into the liquid is supposed to be negligible because of the short time scale.

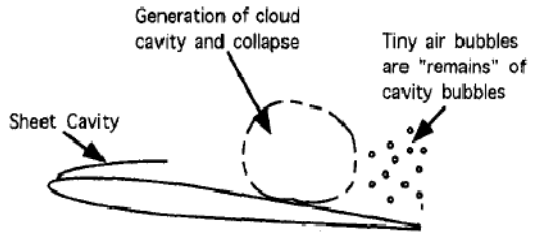

Figure 16 Generation and collapse of cloud cavity (Kato et al. [18])

The impact pressures on the foil surface are then estimated based on a model for an isolated implosion of a single bubble in an infinite space. This model neglects interference effects that occur in bubble clouds (see e.g. Reisman et al. [5]). Furthermore, it neglects diffraction effects from the nearby wall.

By combining the cavity generation rate and the number and size of the bubbles, the impact force/pressure spectrum on the solid surface can be estimated. First, the cavity collapsing region and the ambient pressure for collapse is estimated. Next, the bubble collapsing rate at a certain position on the solid surface should be estimated with the spatial distribution of bubbles. It is however very time consuming to calculate the impact forces and pressure caused by each collapsing bubble. Therefore, it is assumed that only the bubbles in the effective layer can cause impact forces and pressures high enough to damage the solid surface. The trajectory of the bubbles can then be represented by a reference trajectory, see Figure 17. Then, three reference length scales are introduced: bubble layer thickness (h_b), effective layer thickness (h_e) and reference trajectory (h). The effective layer thickness was assumed to be one-tenth of the bubble layer thickness and the reference trajectory is supposed to follow the center of the effective layer, i.e. $h = h_e / 2$.

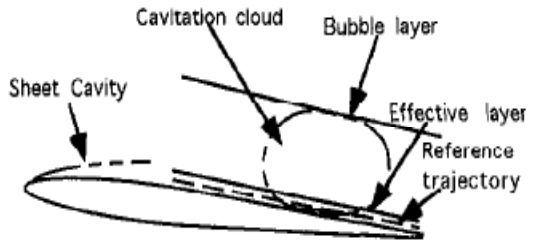

Figure 17 Bubble layer, effective layer, and reference trajectory (Kato et al. [18]).

This model allows for a quantitative prediction of cavitation erosion without using a model test. However, it involves several parameters which were assumed or neglected without confirmation, such as the initial gas pressure inside a bubble, the spatial distribution of collapsing bubbles, the change of ambient pressure around collapsing bubbles, and the interaction of bubbles as well as that between bubbles and the solid wall.

Although the model by Kato et al. [18] is an interesting attempt to capture the process from cavity shedding up to and including the generation of shock waves, the neglects and simplified empirical relations, often derived from model experiments on only one configuration, make the applicability of this model for propellers and rudders highly questionable. This is acknowledged by the authors, who state that "further experimental as well as theoretical verifications of the assumed values (and relations) are essential for the development of the proposed method". Furthermore, the described mechanism lacks the important role of a vortical flow in the focusing of the energy. The reference trajectory for the shed cavities defined in this model seems to differ from the development of shed vortices into horseshoe vortices, as hypothesized in the foregoing.

MODEL BY BARK ET AL. (2004)

The main aim of the work within the European Project EROCAV was to develop a practical tool for the assessment of the risk of erosion on ship propellers and rudders in an early design stage. The observation handbook by Bark et al [2] summarized by Bark et al. in [9], gives a good insight into the complete hydrodynamic process from the early and global development of the erosive cavity to the focused cavity collapse and possible rebound.

The model is built on the notion that erosion is primarily the result of an accumulated energy transfer from macro scale cavities to collapsing cavities close to a solid surface.

The core of the model consists of a number of definitions. A conceptual model is constituted to sharpen the visual interpretation of observations of cavitation processes by high-speed video, and a systematic nomenclature is proposed to describe and classify the cavitation behavior with respect to focusing and the generation of erosion.

The small cavities that result from the focusing cavity are assumed to cause the pitting in the material. They may be considered approximately spherical at the start of the collapse, but later, if close enough to the body surface, develop a high speed micro-jet hitting the solid. This jet, as well as the local pressure wave generated during the collapse, can contribute to the deformation and fatigue of the solid material. It is thereby assumed that either the micro-jet or the pressure wave alone can be the dominating mechanisms, depending on actual conditions. "The most violent collapse of the cavities is associated with the collective collapse of cloud cavitation. This collective behavior consists of a cascading energy transfer from the collapse of the peripheral bubbles to the innermost bubbles whereby the collapse energy is focused into a small volume" [2].

Following the idea of an energy cascade model, a decomposition of the erosive cavitation process is worked out in detail. The natural basis for decomposition of the cavity collapse is the existence of physically identifiable sub processes, the observation of which depends on the observation technique used. With this in mind, the decomposition of the erosive cavitation process is briefly described as follows, following a phenomenological description:

- The creation of a transient, usually travelling, cavity from the global cavity on a propeller blade or similar.
- The main focusing collapse. This is the early collapse motion of the transient cavity that can be observed by the selected recording technique.

- The micro focusing collapse. This is the last part of the collapse, not resolved in detail by high-speed recordings.
- The rebound.

Guidelines for Observation and Analysis

Bark et al [2] provide guidelines to assess the erosiveness from visual observations. They first search for violent rebounds and estimate it's violence. They then advise to attempt to backtrack the cavity to its origin. Alternatively they suggest to directly detect focusing cavities from the global cavity structure. An assessment of the vapor content should be made, where Bark et al. define the quality of a cavity in terms of "glassy", "cloudy" or "mixed". The first qualification referring to a close to 100% vapor fraction cavity, the latter two to significantly smaller vapor ratios. Information on the focusing efficiency can also be obtained from:

- The amount of disintegration
- The acceleration of the collapse motion
- The shape and symmetrie of the collapse motion
- The cyclic behavior of the focusing in relation to forced oscillations, e.g. through the propeller shaft rate.

All the listed points concern mainly the focusing cavity from its early development toward the rebound, the latter event being used as an indicator of a violent collapse. No detailed observation of the micro focusing process is requested, which is identified as a topic for further investigation.

The proposed erosion assessment model can easily be applied on rather large-scale cavities, at a scale which can be predicted by contemporary CFD methods. However, in cases where the erosive cavities are small in size and form part of a complex cavity behavior, application of this model becomes more difficult. It is noted by the authors that in an experimental assessment, the time and costs needed to make useful high-speed video recordings are more limiting than the visual analysis itself. In addition, due to scale effects, lack of experience or full scale correlation it may also happen that the risk of erosion is over-estimated or underestimated. A combination of the visual method and a paint tests is therefore recommended by the authors, possibly supplemented also by noise measurements in the high frequency range.

MODEL BY FORTES PATELLA ET AL. (2004)

Fortes-Patella et al. [3] proposed a physical scenario to describe the mechanism of cavitation erosion (see Figure 18). This model shows us how to evaluate the energy transfer between the cavitating flow and the damage material. It is based on the following phases:

- The collapses of the vapour structures of the cavitating flow
- The emission and the propagation of the pressure wave during the collapse of vapour structures of the cavitating flow (Challier et al. [19])
- The interaction between the pressure waves and the neighbouring solid surface (Fortes-Patella et al. [20])
- The damage of the material exposed to the pressure wave impacts (Fortes-Patella [21])

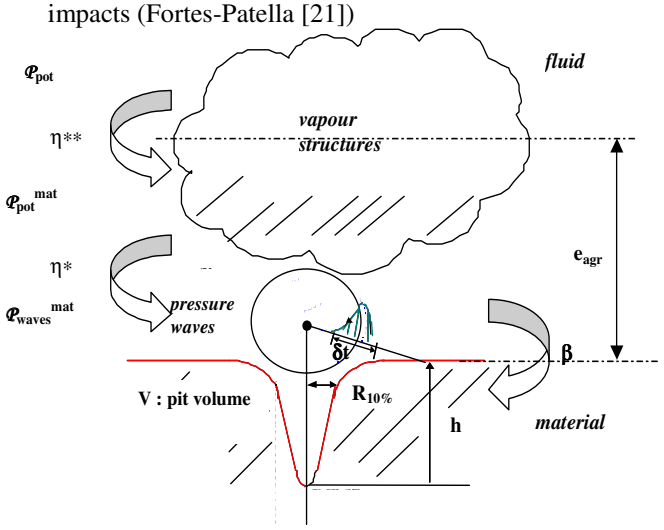

Figure 18 Scheme of the physical scenario based on an energy balance (Fortes Patella et al [3])

Similar as for the model by Bark et al. [2], this cavitation erosion model is based on the concept of the energy cascade, in which the potential power apparent from the macro cavities is converted into acoustic power produced by collapsing clouds of micro bubbles. It is thereby suggested that pressure waves emitted during the collapses of vapor structures are the main source contributing to the cavitation erosion. The emission of the pressure wave can be generated either by spherical bubble or vortex collapses as well as by micro-jet formation. The emitted pressure waves interact with neighboring solid surfaces, leading to material damage. The development of macro cavities, which was taken as input in this model, can either be observed from experiments or calculated using various CFD multiphase methods. Finally, the volume damage rate can be calculated as output from this model.

Instantaneous Potential Power

The instantaneous potential power of the cavitating flow can be derived from a consideration of the macroscopic cavity structure. It is defined by:

$$P_{pot} = \Delta p(\frac{dV_{vap}}{dt}) \quad (5)$$

where $\Delta p = p_\infty - p_{vap}$, p_∞ is the surrounding pressure, p_{vap} is the vapor pressure and V_{vap} is the vapor volume at given time t.

Flow Aggressiveness Potential Power

The flow aggressiveness potential power, derived from the potential power that relates to the erosive aggressiveness before the occurrence of collapse, was given by:

$$p_{pot}^{mat} = \eta^{**} p_{pot} \quad (6)$$

where the energy transfer efficiency η^{**} is a function of the hydrodynamic characteristics(V_{ref} and σ) of the main flow and the distance between the collapse center and the material surface L. The quantity V_{ref} is the reference velocity of the flow, and σ is the cavitation number. This Flow aggressiveness power is influenced by the type, unsteadiness and geometry of the cavitating flow, such as the angle of attack and the shape of the leading edge for a hydrofoil.
It is noted here however, that according to the definition of the potential power P_{pot}, information about the development of cavitation, which can be related to the flow hydrodynamics and the type and geometry of the cavitating flow is already accounted for. Consequently, the most relevant influence factor appears to be the distance between the collapse center and the material surface.

Pressure Wave Power

The pressure wave power applied to the material during the vapor bubble collapse is defined by:

$$p_{waves}^{mat} = \eta^{*} p_{pot}^{mat} \tag{7}$$

where the efficiency η^{*} is suggested to be determined by the collapses of spherical bubbles of vapor and gas. It depends mainly on the change in the surrounding pressure p_{∞} relative to the pressure upon the first generation of cavitation for which the potential power is determined, and the air content in the flow.

Volume Damage Rate

The volume damage rate V_d was measured by a 3D laser profilometer and was related to the flow aggressiveness, referred to as $p_{pot}^{mat} / \Delta S$, by the formula:

$$V_d = \frac{\eta^{*}}{\beta} \frac{p_{pot}^{mat}}{\Delta S} = \frac{p_{waves}^{mat}}{\beta \Delta S} \tag{8}$$

where ΔS is the analyzed sample surface, and β is a mechanical transfer function depending strongly on the characteristics of the material.

An advantage of this model is that it follows the description of the physical energy transfer processes. The reliability of this model depends directly on the assessment of the two efficiencies. However, details on the determination of these efficiencies have not been found in the open literature. The applicability of this model for interpretation of CFD results depends therefore on the reliability of the assessment of these energy transfer ratios. The effectiveness of the focusing process should be represented by these transfer ratios.

MODEL BY DULAR ET AL. (2006)

Dular et al [6] suggest a model for the cavitation erosion process based on the damage caused when a bubble collapses in the vicinity of a solid surface. These single bubbles are supposed to be excited by the shock wave that is emitted from the collapse of a cavitation cloud.

The cavitation erosion model is based on partly theoretical, partly empirical considerations, which are derived from knowledge that was gained during earlier studies of different authors. An obvious correlation between the cavitation structures and cavitation erosion was found through experimental investigations and statistical calculations. Perhaps the most important assumption in the assessment of erosion risk is that the value of the standard deviation of grey level for each position correlates with the magnitude and distribution of damage caused by the cavitation erosion.

The cavitation erosion process is broken down into four different phases, ultimately leading to pit formation (see Figure 19):

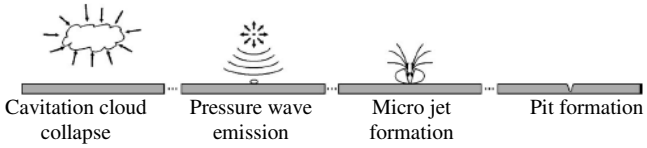

Figure 19 Cavitation Erosion model by Dular et al. [6]

- Collapse of the cavitation cloud causes a shock wave that radiates into the fluid.
- The magnitude of the shock wave is attenuated as it travels toward the solid surface.
- Single bubbles present near the solid surface begin to oscillate and a micro-jet phenomenon will occur if the bubble is close enough to the wall.
- The damage (single pit) is caused by a high velocity liquid jet impacting the solid surface.

The power and consequently the magnitude of the emitted pressure wave are closely related to the velocity of the change of the vapour cloud volume (velocity of cavitation cloud collapse) and to the surrounding pressure. This power term corresponds to the instantaneous potential power P_{pot} defined in the model by Fortes-Patella et al [3].

From acoustical theory, it follows that the amplitude of the emitted pressure wave is proportional to the square root of the acoustic power. Dular et al. consider the pressure difference Δp in the potential power to remain approximately constant during the process, so that the distribution of the mean change in cavitation cloud volume on the hydrofoil reveals the mean distribution of amplitude of the pressure wave that is emitted by the cavitation cloud collapse.

A hypothesis that the standard deviation of the grey level is related to the dynamics of cavitation was made on the basis of previous studies by Dular et al. Based on this hypothesis, they substitute the instantaneous change of the cavitation cloud volume by the standard deviation of the grey level in the experimental observations, which is then related to the power of the emitted pressure wave. “Standard deviation can be used in this manner since it is a function of the change of the grey level in the image, which is a function of the cavitation cloud volume.”

It is interesting to note that the physical process assumed to be responsible for cavitation erosion by Dular et al. is the reverse of the physical process hypothesized in this paper,

where in the latter one initial implosion synchronizes the implosion of a bubble cloud. Another comment on this model is that the erosion aggressiveness is based on the notion that the damage is caused by the impingement of the microjet associated with the implosion of the individual bubbles, whereas in the hypothesized model in this paper, it is argued that the acoustic power that is released from this mechanism is significantly smaller than the acoustic power released from the synchronized bubble cloud collapse. A third comment refers to the use of the standard deviation of pixels as a measure for the time rate of change of the vapor volume. Based on digital postprocessing of high speed video observations, it is our experience that high standard deviations in the grey value at one position do not necessarily refer to the time rate of change of the cavity volume, but may also refer to e.g. the size of the bubbles contained in a transient cavity.

EVALUATION OF MODELS

The models by Bark et al. [2] and Fortes-Patella et al. [3] are based on energy transfer considerations, which have the inherent advantage that details of the collapse process, such as needed e.g. in the model by Kato et al. [18] need no detailed description, other than an energy transfer. This energy transfer process can simply be captured in a semi-empirical transfer ratio. These two models also better match the hypothesized mechanism for cavitation erosion described in this paper.

CONCLUSION

A detailed phenomenological description of the process leading to cavitation erosion from sheet cavitation and vortex cavitation is hypothesized. The hypothesis is based on experiments and observations published in open literature and backed up with four full scale observations discussed in this paper. The process is based on the conversion of potential energy contained in the cavity and a focusing of this energy in space and in time that is governed by ring vortices or horseshoe vortices in case the ring vortices attach to a surface. It is concluded from experiments by Kawanami etal. [1] that horseshoe vortices tend to concentrate the vorticity toward the material surface. It is hypothesized in this paper that this concentrated vorticity forms a mechanism to break a monolithic cavity up into bubbles due to instabilities caused by the high fluid velocities and to concentrate all microbubbles in space by centrifuging out the heavier liquid particles. The radiated shockwaves caused by the implosion of one microbubble is then hypothesized to be sufficient to initiate a synchronized implosion of the cloud of microbubbles in the immediate vicinity.

This process differs from the process described by Bark et al. [2] in the emphasis that is put on the role of concentrated vorticity for the focusing of the potential energy and the breaking up of a monolithic cavity into microbubbles, prior to a synchronized collapse of this microbubble cloud.

A selection of cavitation erosion models available in open literature is reviewed in this paper. It is concluded that the models by Bark et al. [2] and Fortes-Patella et al. [3] appear to offer the best frameworks to be coupled to the mechanisms hypothesized in this paper.

Further work will be directed toward a better understanding of the dynamics of cavitating vortices with respect to radiated acoustic power and shock waves, and toward a further development of the erosion models to close the gap between the output of multiphase RANS codes and the risk of cavitation erosion.

ACKNOWLEDGMENTS

Part of this work has been sponsored by the Cooperative Research Ships, coordinated by MARIN. Financial and moral support is gratefully acknowledged.

REFERENCES

[1] Kawanami, Y., Kato, H., Yamaguchi, H., Maeda, M. and Nakasumi, S. 2002; “Inner Structure of Cloud Cavity on a Foil Section”, JSME International Journal, Series B, Vol 45, No 3

[2] Bark, G., Berchiche, N. and Grekula, M. 2004; “Application of principles for observation and analysis of eroding cavitation – The EROCAV observation handbook”, Edition 3.1

[3] Fortes-Patella, R., Reboud, J.L. and Briancon-Marjollet, L. 2004; “A phenomenological and numerical model for scaling the flow agressiveness in cavitation erosion”, EROCAV Workshop, Val de Reuil

[4] Friesch, J. 2006, Rudder Erosion Damages Caused By Cavitation Proceedings from Sixth International Symposium on Cavitation, Wageningen, The Netherlands

[5] Reisman, G.E., Wang Y.-C. and Brennen, C.E. 1998; Observations of shock waves in cloud cavitation, Journal of Fluid Mechanics, 355, pp255-283

[6] Dular, M, Sirok, B. and Stoffel, B. 2006 ; “Experimental and numerical modelling of cavitation erosion”, Sixth International Symposium on Cavitation, CAV2006, Wageningen

[7] Gavaises, M., Papoulias, D., Andriotis, A. and Giannadakis, E. 2007; “Link between cavitation development and erosion damage in diesel injector nozzles”, Congress on Diesel Fuel Injection and Sprays (SP-2083), SAE International

[8] Hammitt, F. G., 1963, “Observations on Cavitation Damage in a Flowing System”, Trans. ASME, J. of Basic Engineering, pp. 3

[9] Bark, G., Friesch, J., Kuiper, G., Ligtelijn, J.T. 2004 “Cavitation Erosion on Ship Propellers and Rudders”, 9th Symposium on Practical Design of Ships and Other Floating Structures, Luebeck-Travemuende, Germany

[10] Franc, J.P., Michel, J.M. 2004; “Fundamentals of Cavitation”, Kluwer Academic Publishers, Dordrecht

[11] Fujikawa, S. and Akamatsu, T. 1980; “Effects of non-equilibrium condensation of vapor on the pressure wave produced by the collapse of a bubble in a liquid”, Journal of Fluid Mechanics 97, part 3, pp481-512

[12] Oba, R.; “The severe cavitation erosion”, Proc. 2nd International Symp. on Cavitation, Tokyo (Japan), April 5-7, 1998

[13] Foeth, E.J., Van Terwisga, T. and Van Doorne, C. 2008; “On the collapse structure of an attached cavity on a

three dimensional hydrofoil", Journal of Fluids Engineering, Vol 130
[14] Pereira, F., Avellan, F., Dupont, Ph. 1998; "Prediction of Cavitation Erosion: An Energy Approach", Journal of Fluids Engineering, Vol. 120
[15] Schmidt, S.J., Sezal, I.H., Schnerr, G.H. and Thalhamer, M. 2007; Proc. of the 8th Int. Symposium on Experimental and Computational Aerothermodynamics of Internal Flows, Lyon
[16] Kuiper, G. 2001 "New developments around sheet and tip vortex cavitation on ships'propellers", Proc. CAV2001 – Fourth International Symposium on Cavitation, Pasadena
[17] Moeny, M., Weldon, M., Stinebring, D., Straka, W. and Pierzga, M. 2008; "Cavitation damage from an induced secondary vortex", Proc. of FEDSM2008, 2008 ASME Fluids Engineering Conference, Jacksonville, USA
[18] Kato, H., Konno, A., Maeda, M., Yamaguchi, H. 1996 "Possibility of quantitative prediction of cavitation erosion without model test", Journal of Fluids Engineering, Vol 118
[19] Challier, G., Fortes Patella, R., and Reboud, JL., 2000, "Interaction Between Pressure Waves and Spherical Cavitation Bubbles : Discussions about cavitation erosion mechanism", Proceedings of the 2000 ASME Fluids Engineering Summer Conference, Boston, Massachusetts.
[20] Fortes Patella, R., Challier, G., Reboud, JL., and Archer, A., 2001, "Cavitation erosion mechanism: numerical simulations of the interaction between pressure waves and solid boundaries", Proceedings of CAV 2001 Symposium, Pasadena.
[21] Fortes-Patella, R., and Reboud, JL., 1998, "A New Approach to Evaluate the Cavitation Erosion Power", Journal of Fluid Engineering , Transactions of the ASME, Vol. 120, June 1998.